Optimum Salt-Gradient Solar Pond in Jordan

Mohammed Awwad Al-Dabbas
Mutah University, Karak, Jordan

ABSTRACT

A brief description of the various models of solar ponds, their main objectives and their development, including a detailed review of the world wide activities in this field are given. Such models usually give an accurate representation of seasonal variation in pond performance and help understand the effect of varying pond designs parameters. In this work, a mathematical model was developed for a one dimension transient conduction heat transfer with heat generation in a Salt Gradient Solar Pond (SGSP). The model incorporates an attenuation model for solar radiation through the water body as proposed by Brinkworth and Hawalder. The model includes a detailed representation of the loss from the pond service by using average daily and monthly meteorological data for the Dead Sea region, in middle Jordan (31.03°N lat) and (348°E long). The relationship derived by the model is solved numerically by employing an implicit finite difference approach, and incorporating initial and boundary conditions and load variation. Next, the stability and convergence of solar pond is examined over a wide range of depth difference and time difference. Finally, numerical results confirm that solar heating In the SGSP is considerably more pronounced during the hot seasons than during the cold ones.

Key words: salt gradient, solar pond, math modeling, finite difference, heating load

INTRODUCTION

Jordan is a developing non-oil producing country. Its basic energy requirements are obtained from imported oil and petroleum products from different sources. Domestic natural gas covers only 3-4% of the

Kingdom's energy need. Renewable energy applications in Jordan includes solar water heaters of more than 300,000 units, solar photovoltaic of more than 200 kW peak, wind farms of 1.5 MW, hydropower of 5 MW and biogas of 3 MW. The total contribution of renewable energy in Jordan is less than 2% of the total energy mix. Oil shale reserves in Jordan are estimated at 40 billion tons, containing 40 billion barrels of oil. This strategic source of energy could be adequate to cover Jordan's current energy requirements for hundreds of years if the resources are to

Also known as salinity gradient solar pond (SGSP), a solar pond collects and stores solar energy. See Figure 1. It is an alternative way of harnessing solar energy to heat water which in turn can be used (a) to generate electricity, (b) to obtain potable water through desalinization or (c) to recover valuable salts. A salt gradient solar pond is a hydraulic system involving heat and mass transfer. Such an approach to harness solar energy has been shown to be economically viable in a large commercial scale [1-3].

A solar pond is being used to evaporate 90 million m^3 per year of the Dead Sea Water for Potash Production. This amount of solar evaporation is equivalent to about 5 million tons of oil per year. Around 3% of the total population in Jordan occupies 41% of the total area of Jordan. This part represents the rural and remote areas, which lack electric and water networks [4-6].

Figures (2-4) show the temperature & relative humidity; number of the day light hours & sun set hour angle, and the solar incident radiation in Amman city in 2009.

Solar energy may become an important contributor to the total energy supply. A solar pond, which collects and stores solar energy, is a shallow body of water in which a downward salinity gradient is established to counteract the buoyancy induced by absorption of solar radiation (Fig. 1). The denser fluid at the bottom of the pond is heated to high temperatures, thus collecting and storing solar energy. The integration of solar pond into a total energy system requires knowledge of their performance under different modes of operation and control. Accurate and efficient analytical modeling is a key factor in making overall system simulation possible. While many analytical models exist in the 1iterature, there are no guidelines as to their accuracy, computational efficiency and simplicity [7-9].

In this article, a review of the work published in the solar ponds

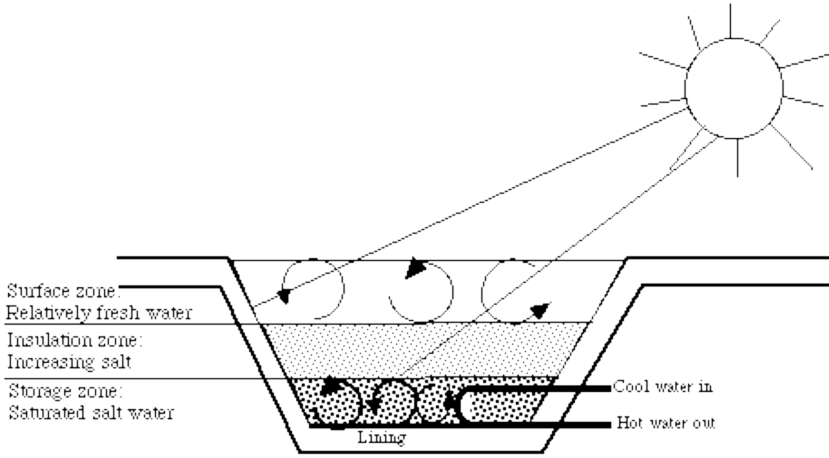

Figure 1. Schematic of a Salt Gradient Solar Pond

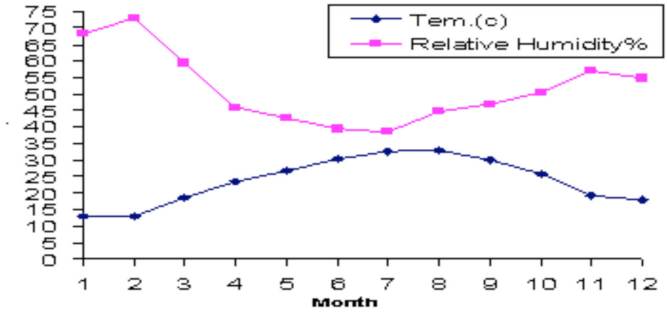

Figure 2. Temperature & Relative Humidity of Amman City in 2009

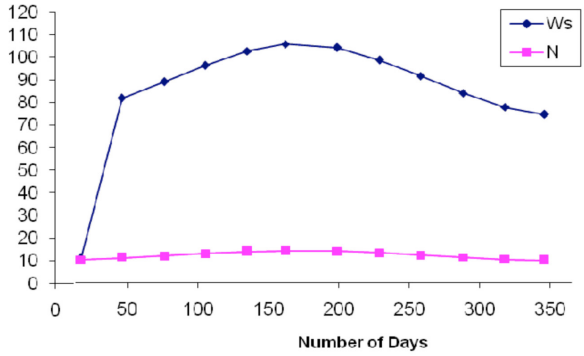

Figure 3. Number of the day light hours & sun set hour angle in Amman city in 2009

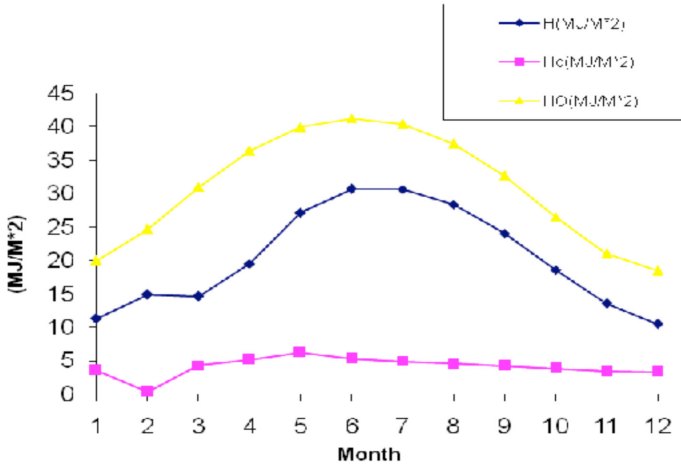

Figure 4. The solar incident radiation in Amman city in 2009

modeling and simulation literature is presented. Selected advanced models were studied in depth. Next, an advanced model is applied to a SGSP for the weather conditions of Jordan. However, to provide the proper perspective for the present work, a review of the literature is presented first.. Research needs and method of approach have been discussed in references [10-11].

Numerical modeling of solar ponds has been reported by many investigators to predict the temperature and salinity profiles in the pond, as well as the prediction of the stability of the solar ponds. Most of these investigations make use of a one dimensional model and use either finite elements or finite difference methods to solve such models [12]. This paper focuses on a one-dimension transient conduction salt gradient solar pond SGSP, with heat generation. The attenuation model for the solar radiation through the water body proposed by Brinkworth and Hawalder was incorporated to the underlying model. The model provides detailed representation of the loss from the pond service and uses daily and monthly averaged local available meteorological data for Dead Sea region in the middle of Jordan (31.03°N lat) and (348°E long).The relationship derived are solved numerically by employing an implicit finite difference approach with a greater freedom to incorporate initial and boundary condition and load variation [13].

The mathematical formulation for the thermal process in a salt-gradient solar pond was derived by assuming a one-dimensional unsteady

conduction heat transfer with heat generation. Note this assumption presupposes a large pond with negligible side effects. The analysis was performed on the basis of a differential formulation approach. This necessitated the introduction of a volume element of a differential length ΔZ, along the depth of the pond as shown in Figure 1. The resulting formulation was then arranged in a backward implicit finite difference using as a basis the nodal diagram shown in Figure 5. Notice in this figure the Upper Convective Zone (UCZ), the Non-Convective Zone (NCZ) and the Lower Convective Zone (LCZ).

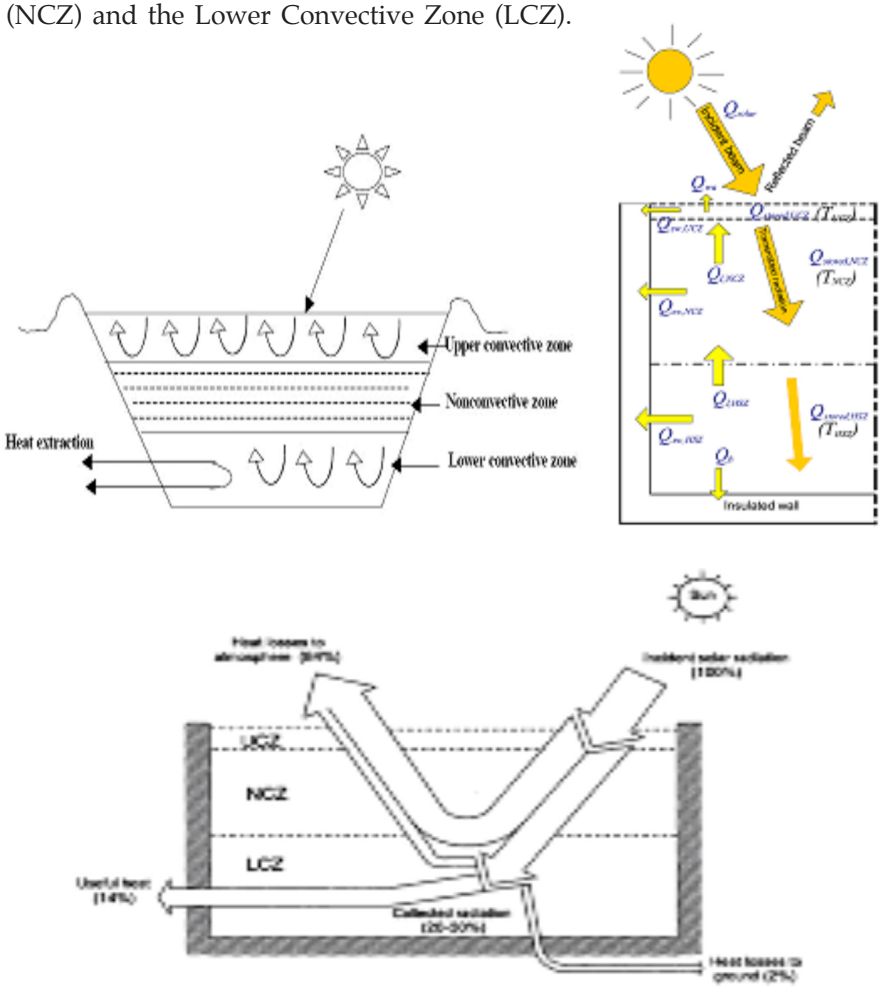

Figure 5. Nodal diagram of the solar pond. Note the Upper Convective Zone (UCZ), Non-Convective Zone (NCZ) and the Lower Convective Zone (LCZ)

The computer program which executes the math model is operated with a one month time step. The input meteorological data include: (a) mean hourly monthly solar radiation incident upon a horizontal surface, (b)air temperature, (c) air speed, and (d) the rate of evaporation for Dead Sea in the middle of Jordan (latitude 31.03°N).

THERMAL ENERGY BALANCE OF THE POND

Figure 5 shows a large pond with neglected edge losses, the heat balance to an element dZ can be written per a unit area in the form:

$$q_z - q_{z+dz} + H_z - H_{z+dz} = \frac{\partial U}{\partial t} \tag{1}$$

Where,

$$q_z = -k\frac{dT}{dZ} \qquad \text{and} \qquad \frac{\partial U}{\partial t} = \rho C \frac{\partial T}{\partial t}\Delta Z \tag{2}$$

Where,

Substituting for equation (2), in equation (1) results in

$$\frac{\partial T}{\partial t} = \frac{k}{\rho C}\frac{\partial^2 T}{\partial Z^2} - \frac{1}{\rho C}\frac{\partial \mathrm{H}_z}{\partial Z} \tag{3}$$

The total radiation H_z, consists of two components, one due to the transmitted radiation from the surface, H_i, and the other, H_r, due to the reflection at the bottom of the pond. Hence, the total radiation at a depth Z from the surface is given by [14]:

$$\mathrm{H}_z = (\mathrm{H}_i)_z + (\mathrm{H}_r)_z \tag{4}$$

But $$(\mathrm{H}_i)_z = \mathrm{H}_s(1-F)\exp\left(\frac{-\mu(\mathrm{Z}-\delta)}{\cos\theta_t}\right) \tag{5}$$

And, $$(\mathrm{H}_r)_z = \mathrm{H}_s(1-F)(1-\alpha)\exp\left(\frac{-\mu(D-\delta)}{\cos\theta_r}\right)\exp\left(\frac{-\mu(D-Z)}{\cos\theta_r}\right) \tag{6}$$

Differentiating equation (4) regarding equations (5,6) yields:

$$\frac{\partial H_z}{\partial Z} = \frac{H_s(1-F)\mu}{\cos\theta_r}\exp\left(\frac{-\mu(Z-\delta)}{\cos\theta_r}\right) + \frac{H_s(1-F)(1-\alpha)\mu}{\cos\theta_r}\exp\left(\frac{-\mu(D-\delta)}{\cos\theta_r}\right)\exp\left(\frac{\mu Z}{\cos\theta_r}\right) \tag{7}$$

Substituting equation (7) in equation (3) yields [15]:

$$\frac{\partial T}{\partial t} = \frac{K}{\rho C}\frac{\partial^2 T}{\partial Z^2} + \frac{1}{\rho C}\left[\frac{H_s(1-F)\mu}{\cos\theta_r}\exp\left(\frac{-\mu(Z-\delta)}{\cos\theta_r}\right) + \frac{H_s(1-F)(1-\alpha)\mu}{\cos\theta_r}\exp\left(\frac{-\mu(2D-\delta)}{\cos\theta_r}\right)\exp\left(\frac{\mu Z}{\cos\theta_r}\right)\right] \tag{8}$$

Initial Condition [16]:

It is assumed that the initial temperature is equal to the ambient temperature at the time we initiate the operation of the pond, and it is constant over the full depth.

Boundary Condition at the Surface (i.e. at Z=0):

As seen in Figure 5, this condition can be formulated by applying the energy conservation at the surface as follows:

$$q_{cond}\big|_{z=z1} = q_{loss} + H_s - H_{z1} = \rho C Z_1 \frac{\partial T_s}{\partial t} \tag{9}$$

But $$q_{loss} = q_r + q_c + q_o \tag{10}$$

Where: $$q_r = \varepsilon\sigma\left[(T_s + 273.15)^4 - (T_{sky} + 273.15)^4\right] \tag{11}$$

$$q_c = h_c(T_s - T_{amb}) \quad , \quad h_c = 5.7 + 3.8V \tag{12}$$

The evaporation heat transfer $$q_e = 27.732\dot{e} \tag{13}$$

Substituting in equation (9-13) yields:

$$\frac{\partial T_s}{\partial t} = \frac{1}{\rho C Z_1}\left[\begin{array}{l} k\frac{\partial T_s}{\partial Z} - \varepsilon\sigma\left(\left(T_s + 273.15\right)^4 - \left(T_{sky} + 273.15\right)^4\right) - \\ hC\left(T - T_{amb}\right) - 27.732\dot{e} + H_s - H_s(1-F)\exp\left(\frac{-\mu\left(Z_1 - \delta\right)}{\cos\theta_r}\right) + \\ H_s(1-F)(1-\alpha)\mu\exp\left(\frac{-\mu\left(D-\delta\right)}{\cos\theta_r}\right)\exp\left(\frac{-\mu\left(D-Z_1\right)}{\cos\theta_r}\right) \end{array}\right] \quad (14)$$

Bottom Boundary Condition (i.e. at Z=Z2):

Applying the energy conservation on the LCZ yields

$$H_{z2} - q_{cond,z=z2} - q_g - q_{Ld} = \rho C D_s \frac{\partial T_b}{\partial t} \quad (15)$$

Following the same procedure yields:

$$\left.\frac{\partial T_b}{\partial t}\right| = \frac{H_s(1-F)}{\rho C D_s}\exp\left(\frac{-\mu\left(Z_2-\delta\right)}{\cos\theta_r}\right) - \frac{H_s(1-F)(1-\alpha)}{\rho C D_s}\exp\left[\frac{-\mu\left(D-\delta\right)}{\cos\theta_r}\right]\exp\left[\frac{-\mu\left(D-Z_2\right)}{\cos\theta_r}\right] - \frac{k}{\rho C D_s}\left.\frac{\partial T}{Z}\right| - \frac{U_{lg}}{\rho C D_s}\left(T-T\right) - \frac{q_{Ld}}{\rho C D_s} \quad (16)$$

ENERGY CONSERVATION FOR NCZ

Equation (8) can be written in finite difference form as:

$$T_{i,j} - T_{i,j-1} = \frac{\Delta t k_i}{\rho_i C_i \Delta Z^2}\left(T_{i+1,j} - 2T_{i,j} + T_{i-1,j}\right) + \frac{\Delta t(1-F)\mu \mathrm{H}s_j}{\rho_i C_i \cos\theta_{r_j}}\exp\left[\frac{-\mu\left(i\Delta Z + \mathrm{Z}_{1-\delta}\right)}{\cos\theta_{r_j}}\right] + \frac{\Delta t(1-F)(1-\alpha)\mu \mathrm{H}s_j}{\rho_i C_i \cos\theta_{r_j}}\exp\left[\frac{-\mu(2D-\delta)}{\cos\theta_{r_j}}\right]\exp\left[\frac{\mu(i\Delta Z + \mathrm{Z}1)}{\cos\theta_{r_j}}\right] \quad (17)$$

Where, the subscripts i and j denote position and time, respectively. Next, Equation (17) can be rearranged in the form:

$$\left(\frac{-\Delta t\cdot k_i}{\rho_i C_i \Delta Z^2}\right)T_{i-1,j}-\left(1+\frac{2\Delta t\cdot k_i}{\rho_i C_i \Delta Z^2}\right)T_{i,j}+\left(\frac{-\Delta t\cdot k_i}{\rho_i C_i \Delta Z^2}\right)T_{i,j}=$$
$$T_{i,j-1}+\frac{\Delta t\,(1-F)\,\mu \mathrm{H}s_j}{\rho_i C_i\cos\theta_{r_j}}\exp\left(\frac{-\mu\,(i\,\Delta Z+\mathrm{Z}_1-\delta)}{\cos\theta_{r_j}}\right)+ \qquad (18)$$
$$\frac{\Delta t\,(1-F)(1-\alpha)\mu \mathrm{H}s_j}{\rho_i C_i\cos\theta_{r_j}}\exp\left(\frac{-\mu\,(2D+\mathrm{Z}_1-\delta)}{\cos\theta_{r_j}}\right)\exp\left(\frac{\mu\,(i\,\Delta Z+\mathrm{Z}_1)}{\cos\theta_{r_j}}\right)$$

ENERGY CONSERVATION FOR UCZ, "SURFACE TEMPERATURE"

Introducing equation (16) in the numerical form yields:

$$\frac{\Delta t\,(1-F)(1-\alpha)\mathrm{H}s_j}{\rho_1 C_1 \mathrm{Z}_1}\exp\left(\frac{-\mu(D-\delta)}{\cos\theta_{r_j}}\right)\exp\left(\frac{-\mu(D-\mathrm{Z}_1)}{\cos\theta_{r_j}}\right)+$$
$$\frac{\Delta t\cdot k_1}{\rho_1 C_1 \mathrm{Z}_1\Delta Z}(\mathrm{T}_{1,j-1}-\mathrm{T}_{s,j})-\frac{\Delta t}{\rho_1 C_1 \mathrm{Z}_1}\left[h_{c_j}(\mathrm{T}_{s,j}-\mathrm{T}_{amb_j})+\varepsilon\sigma\left(\left(\mathrm{T}_{s,j-1}+273.15\right)^4-\left(\mathrm{T}_{sky}+273.15\right)^4\right)+27.752e\right] \qquad (19)$$

Equation (19) can be rearranged in the form:

$$\left(1+\frac{\Delta t\cdot k_1}{\rho_1 C_1 \mathrm{Z}_1\Delta Z}+\frac{\Delta t\cdot h_{s_j}}{\rho_1 C_1 \mathrm{Z}_1}\right)\mathrm{T}_{s,j}=\mathrm{T}_{s,j-1}+\mathrm{A}+\frac{\Delta t\cdot k_1}{\rho_1 C_1 \mathrm{Z}_1\Delta Z}\mathrm{T}_{1,s-1}-$$
$$\frac{\Delta t\cdot h_{c_j}}{\rho_1 C_1 \mathrm{Z}_1}\mathrm{T}_{amb_j}-\frac{\Delta t\cdot\varepsilon\cdot\sigma}{\rho_1 C_1 \mathrm{Z}_1}\left(\mathrm{T}_{s,j-1}+273.15\right)^4+\frac{\Delta t\cdot\varepsilon\cdot\sigma(\mathrm{T}_{sky}+273.15)}{\rho_1 C_1 \mathrm{Z}_1}-\frac{27.732}{\rho_1 C_1 \mathrm{Z}_1}e$$

Where A is the first three terms in the right-hand side of equation (20)

Let $$D_1=1+\frac{\Delta t\cdot k_1}{\rho_1 C_1 \mathrm{Z}_1\Delta Z}+\frac{\Delta t\cdot h_{c_j}}{\rho_1 C_1 \mathrm{Z}_1} \qquad (21)$$

And D2 to be the R.H.S. of equation (4) then:

$$\mathrm{T}_{s,j}=\frac{D_2}{D_1} \qquad (22)$$

But according to equation (19)

$$T_{1,j} - T_{1,j-1} = \frac{\Delta t \cdot k_1}{\rho_1 C_1 \Delta Z^2}\left(T_{s,j} - 2T_{1,j} + T_{2,j}\right) + \frac{\Delta t\,(1-F)\mu H s_j}{\rho_1 C_1 \cos\theta_{r_j}} \exp\left(\frac{-\mu\left(\Delta Z + Z_1 - \delta\right)}{\cos\theta_{r_j}}\right)$$
$$\frac{\Delta t\,(1-F)(1-\alpha)\mu H s_j}{\rho_1 C_1 \cos\theta_{r_j}} \exp\left(\frac{-\mu\left(2D - \delta\right)}{\cos\theta_{r_j}}\right) \exp\left(\frac{\mu\left(\Delta Z + Z_1\right)}{\cos\theta_{r_j}}\right) \tag{23}$$

Equation (23) can be arranged in the form:

$$\left(1 + \frac{2\Delta t \cdot k_1}{\rho_1 C_1 Z_1 \Delta Z}\right) T_{1,j} + \left(\frac{-\Delta t \cdot k_1}{\rho_1 C_1 \Delta Z^2}\right) T_{2,j} = T_{1,j-1} + \frac{\Delta t\,(1-F)\mu H s_j}{\rho_1 C_1 \cos\theta_{r_j}} \exp\left(\frac{-\mu\left(\Delta Z + Z_1 - \delta\right)}{\cos\theta_{r_j}}\right) +$$
$$\frac{\Delta t\,(1-F)(1-\alpha)\mu H s_j}{\rho_1 C_1 \cos\theta_{r_j}} \exp\left(\frac{-\mu\left(2D - \delta\right)}{\cos\theta_{r_j}}\right) \exp\left(\frac{\mu\left(\Delta Z + Z_1\right)}{\cos\theta_{r_j}}\right) + \frac{\Delta t \cdot k_1}{\rho_1 C_1 \Delta Z^2} \tag{24}$$

Where Ts,j can be obtained according to equation (22).

ENERGY CONSERVATION OF THE LCZ

Introducing equation (19) in the numerical form yields:

$$T_{n,j} - T_{n,j-1} = \frac{\Delta t\,(1-F) H s_j}{\rho_n C_n D s} \exp\left(\frac{-\mu\left(Z_2 - \delta\right)}{\cos\theta_{r_j}}\right) - \frac{\Delta t\,(1-F)(1-\alpha) H s_j}{\rho_n C_n D s} *$$
$$\exp\left(\frac{-\mu\left(D - \delta\right)}{\cos\theta_{r_j}}\right) \exp\left(\frac{-\mu\left(D - Z_2\right)}{\cos\theta_{r_j}}\right) - \frac{k_n \cdot \Delta t}{2\rho_n C_n D s \Delta Z}\left(T_{a+1,j} - T_{a-1,j}\right) -$$
$$\frac{U_{Lg}\Delta t\left(T_{n,j} - T_{gw}\right)}{\rho_n C_n D s} - \frac{q_{Ld}\Delta t}{\rho_n C_n D s} \tag{25}$$

By arranging the above equation

$$T_{n,j} - T_{n,j-1} = \frac{\Delta t\,(1-F) H s_j}{\rho_n C_n D s} \exp\left(\frac{-\mu\left(Z_2 - \delta\right)}{\cos\theta_{r_j}}\right) - \frac{\Delta t\,(1-F)(1-\alpha) H s_j}{\rho_n C_n D s} *$$
$$\exp\left(\frac{-\mu\left(D - \delta\right)}{\cos\theta_{r_j}}\right) \exp\left(\frac{-\mu\left(D - Z_2\right)}{\cos\theta_{r_j}}\right) - \frac{k_n \cdot \Delta t}{2\rho_n C_n D s \Delta Z} T_{n+1,j} + \frac{k_n \cdot \Delta t}{2\rho_n C_n D s \Delta Z} T_{n-1,j}$$
$$- \frac{U_{Lg}\Delta t}{\rho_n C_n D s} T_{n,j} + \frac{U_{Lg}\Delta t \cdot T_{gw}}{\rho_n C_n D s} - \frac{q_{Ld}\Delta t}{\rho_n C_n D s} \tag{26}$$

Substituting for i=n in equation (1) yields:

$$T_{n,j} - T_{n,j-1} = \frac{\Delta t \cdot k_n}{\rho_n C_n \Delta Z^2}\left(T_{n+1,j} - 2T_{n,j} + T_{n-1,j}\right) + \frac{\Delta t(1-F)\mu Hs_j}{\rho_n C_n \cos\theta_{r_j}} \exp\left(\frac{-\mu(Z_2-\delta)}{\cos\theta_{r_j}}\right) + \frac{\Delta t(1-F)(1-\alpha)\mu Hs_j}{\rho_n C_n \cos\theta_{r_j}} \exp\left(\frac{-\mu(2D-\delta)}{\cos\theta_{r_j}}\right)\exp\left(\frac{\mu Z_2}{\cos\theta_{r_j}}\right) \quad (27)$$

$$T_{n+1,j} = \frac{\rho_n C_n \Delta Z^2}{\Delta t \cdot k_n}[T_{n,j} - T_{n,j-1} + \frac{2\Delta t \cdot k_n}{\rho_n C_n \Delta Z^2} T_{n,j} - \frac{\Delta t \cdot k_n}{\rho_n C_n \Delta Z^2} T_{n-1,j} - \frac{\Delta t(1-F)\mu Hs_j}{\rho_n C_n \cos\theta_{r_j}} \exp\left(\frac{-\mu(Z_2-\delta)}{\cos\theta_{r_j}}\right) - \frac{\Delta t(1-F)(1-\alpha)\mu Hs_j}{\rho_n C_n \cos\theta_{r_j}} \exp\left(\frac{-\mu(2D-\delta)}{\cos\theta_{r_j}}\right)\exp\left(\frac{\mu Z_2}{\cos\theta_{r_j}}\right) \quad (28)$$

Or,

$$T_{n+1,j} = \frac{\rho_n C_n \Delta Z^2}{\Delta t \cdot k_n} T_{n,j} - \frac{\rho_n C_n \Delta Z^2}{\Delta t \cdot k_n} T_{n,j-1} - T_{n-1,j} \frac{\Delta Z^2(1-F)\mu Hs_j}{k_n \cos\theta_{r_j}} \exp\left(\frac{-\mu(Z_2-\delta)}{\cos\theta_{r_j}}\right) - \frac{\Delta Z^2(1-F)(1-\alpha)\mu Hs_j}{k_n \cos\theta_{r_j}} \exp\left(\frac{-\mu(2D-\delta)}{\cos\theta_{r_j}}\right)\exp\left(\frac{\mu Z_2}{\cos\theta_{r_j}}\right) \quad (29)$$

Substituting equation (13) in equation (10) yields:

$$\left(1+\frac{\Delta Z}{2D_s} + \frac{\Delta t \cdot k_n}{\rho_n C_n \Delta Z} + \frac{U_{Lg}\Delta t}{\rho_n C_n D_s}\right) T_{n,j} - \left(\frac{k_n \cdot \Delta t}{\rho_n C_n Ds \Delta Z}\right) T_{n-1,j} = \left(1+\frac{\Delta Z}{2D_s}\right) T_{n,j-1} + \frac{\Delta t(1-F)Hs_j}{\rho_n C_n D_s} \exp\left(\frac{-\mu(Z_2-\delta)}{\cos\theta_{r_j}}\right) - \frac{\Delta t(1-F)(1-\alpha)\mu Hs_j}{\rho_n C_n D_s} \exp\left(\frac{-\mu(2D-\delta)}{\cos\theta_{r_j}}\right)\exp\left(\frac{-\mu D_s}{\cos\theta_{r_j}}\right) + \frac{\Delta t \Delta Z(1-F)\mu(1-\alpha)Hs_j}{2\rho_n C_n D_s \cos\theta_{r_j}} \exp\left(\frac{-\mu(2D-\delta)}{\cos\theta r_j}\right)\exp\left(\frac{\mu Z_2}{\cos\theta r_j}\right) - \frac{q_{Ld}\Delta t}{\rho_n C_n D_s} + \frac{U_{Lg}\Delta t \cdot T_{gw}}{\rho_n C_n D_s} \quad (30)$$

Thus we will reach to AT = B, The matrix A can be represented as:

$$A = \begin{bmatrix} 1+2\lambda_1 & -\lambda_1 & & & & & \\ -\lambda_2 & 1+2\lambda_2 & -\lambda_2 & & & & \\ & & -\lambda_i & 1+2\lambda_i & -\lambda_i & & \\ & & & & & C_2 & C_1 \end{bmatrix}$$

Where,

$$\lambda_i = \frac{\Delta t\ \kappa_i}{\rho_i C_i \Delta Z^2}\ ,\ C_1 = \frac{k_n\ \Delta t}{\rho_n D_s C_n \Delta Z}\ ,$$

$$C_2 = 1 + \frac{\Delta Z}{2D_s} + \frac{k_n\ \Delta t}{\rho_n D_s C_n \Delta Z} + \frac{U_{Lg} \Delta t}{\rho_n C_n D_s}$$

And B is the vector consists of the Right Hand Side of theses equations solving equation (15) requires appropriate numerical technique to inverse the matrix A.

RESULTS AND DISCUSSION

In this work, a one-dimensional math model of salt diffusion within the solar pond has been presented and discussed. The equation obtained for the model has been solved numerically by using the finite difference method, to simulate a transient [17]. Based on the numerical approach a computer program was written in MATLAB to investigate the effect of the various parameters on transient thermal performance of the solar pond.

The cyclic behavior of the storage zone can be referred to the annual variation of varies component of the LCZ energy balance illustrated in Figure 4; a net storage energy q_s is positive during the season except for the period between mid-December and mid-February, when the conductive loss the q_{Lc} plus the ground loss q_g plus the extracted q_{Ld} excites the energy reaching the lower convective zone.

The monthly average ground loss is 10 kWhr/m^2 with a maximum value of about 14 kWhr/m^2 in September. Heat transfer by conduction from LCZ to NCZ is predicted for the period from mid august to march in the following g year with a maximum of about 5 kWh/m^2 in December while a heat gain from the NCZ into the LCZ is a achieved during the reminder of the season.

Figure 7 shows a series of temperature profiles for the full depth of the solar pond and for the difference time during the season. As assumed as the NCZ and LCZ are isothermal the profile within the NCZ is non-linear. This has the positive effect of the reducing temperature gradient as the inter face between LCZ and NCZ.

The heat loss by conduction from the storage zone upward to gra-

dient zone, contributes strongly in solar pond radiation. The boundary temperature gradient is approximately zero in March and negative in June and positive in September this may explain well the annual behavior of the heat transfer by conduction at the interface between LCZ and NCZ as illustrated in figure 7.

Effect of the thickness of the non-convicting zone (d):

Once the thickness of the UCZ has been fixed, the thickness of the non-convective zone (NCZ) is important because of the trade off between an increase in the thermal insulation with a concurrent decrease in the solar radiation penetrating into the storage zone as the thickness increases, i.e. if the NCZ which serves as an insulating layer is thin, the upward heat loss by conduction becomes the dominant, causing the storage to be low. On the other hand, an increase of the thickness of NCZ would increase the amount of solar radiation absorbed in its path through the bond, therefore, reducing the radiation reaching the storage zone, and the storage temperature will be again low.

Figure 7 shows that the optimum thickness of the NCZ is 1.0m on the basis of the requirement of highest mean annual storage temperature (71.5 C for 1.5 LCZ).

The Effect of the lower convective zone (Ds):

The thermal performance of the solar pond is analyzed to investigate the effect of increasing the thickness of the storage zone (LCZ). Five computer simulation runs were made in which the thickness of the LCZ was increased from 0.5 to 5m. the results of cyclic storage temperature are plotted in Figure 8, the 1.0m LCZ reached a temperature of 80 C after 5 months from the beginning of the simulation on March, the 0 and 5m storage zones reached the same temperature in about 4.5 and 5 months, respectively, which means that the small thickness leads to m.

Figure 9 shows that the average annual storage temperature is slightly affected by the thickness of the LCZ. However, the maximum temperature of the LCZ varied inversely with its depth. The low maximum temperature in the deep LCZ, results simply because the absorbed energy heats a large volume of brine per unit surface area more than the case of the shallow LCZ, or in other word because of greater heat capacity of a zone of larger depth. The higher minimum temperature in the deeper storage zone, results due to the larger thermal mass within the LCZ, which in turn, results in lower rate of cooling.

The lost energy from the LCZ; is nearly independent of LCZ thickness, but a slight dependent would be expected if the side walls loss was taken in consideration.

The effect of load profile q ld:

The load patter has a strong influence on the temperature profile of the pond and it should be such that not only the maximum possible amount of heat is extracted but also the load temperature requirements are satisfied [9]. In other words, temperature and load matching between a particular application and solar pond thermal performance is of obvious design importance. The seasonal thermal performance of the pond is sensitive to the total energy extraction and to when extraction stars.

The annual average storage zone temperature depends highly on the rate of heat extraction q ld The non-convective zone thickness and annual average storage zone temperature is depicted in Figure 10. This figure shows the effect of NCZ thickness on the average temperature with q ld as a parameter, It also shows that, for every value of q ld there exists an optimum thickness for the NCZ which yields the highest performance of the pond, and it is clear that this thickness is increasing with the decreasing of the applied load.

Figure 11 shows that as the extraction rate (i.e. a collection efficiency) is increasing, the solar pond capability to store more energy increases too.

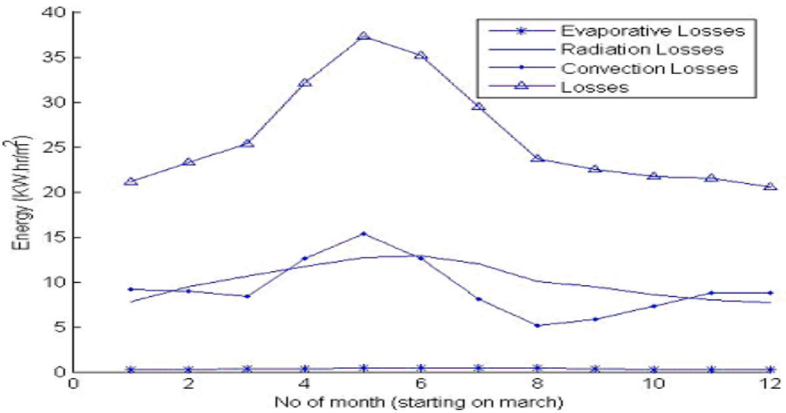

Figure 6. Annual energy balance for the LCZ

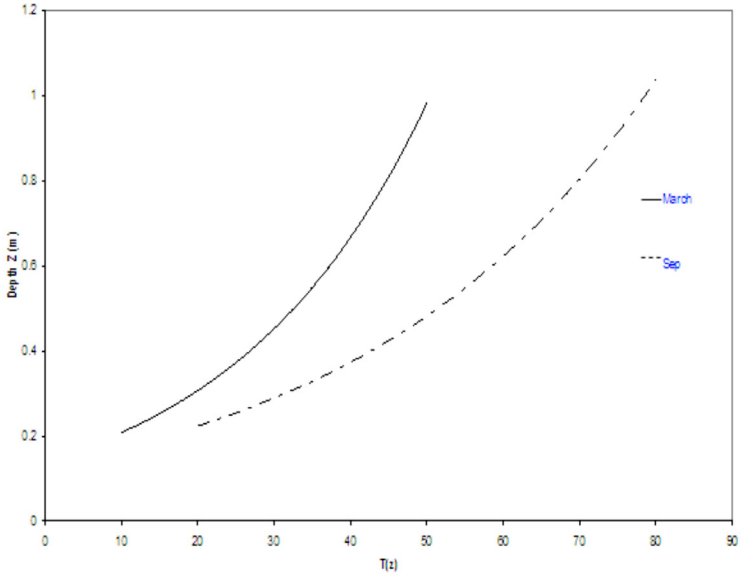

Figure 7. The temperature distribution within the solar pond (Z1=0.2m, D=1.0, μ=1.0m^{-1}, Ds=1.5m)

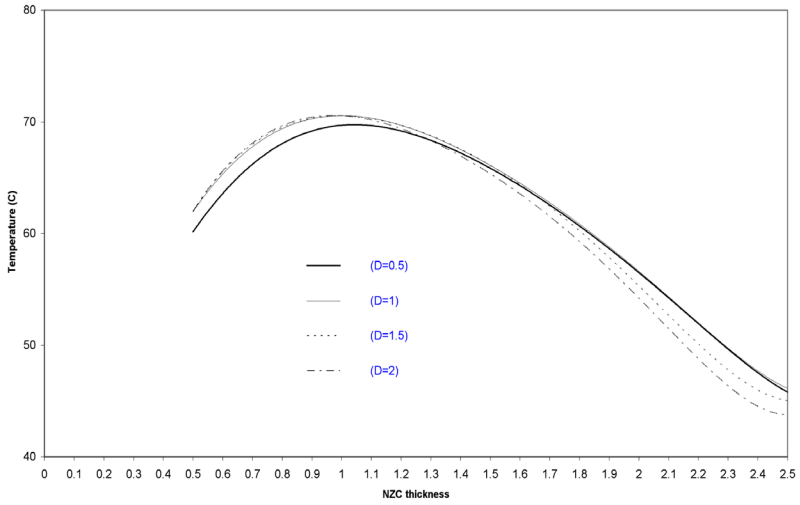

Figure 8. The average annual storage temp vs. NCZ thickness

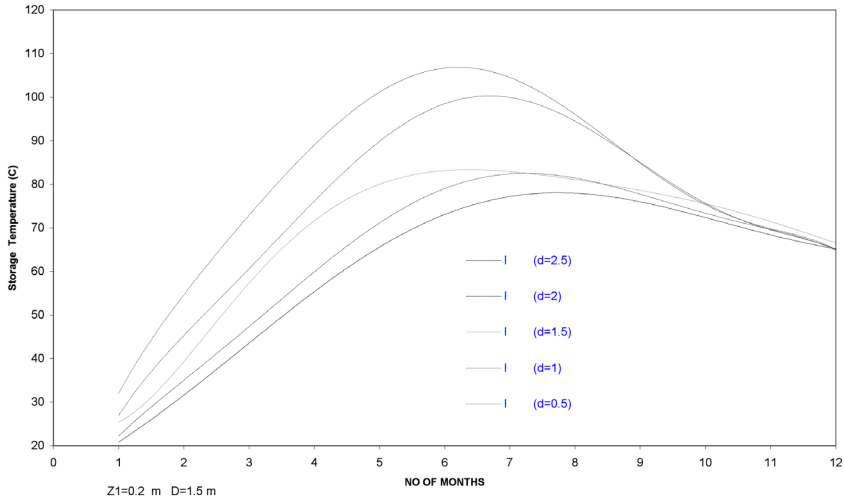

Figure 9. The average annual storage zone temperature vs. LCZ thickness

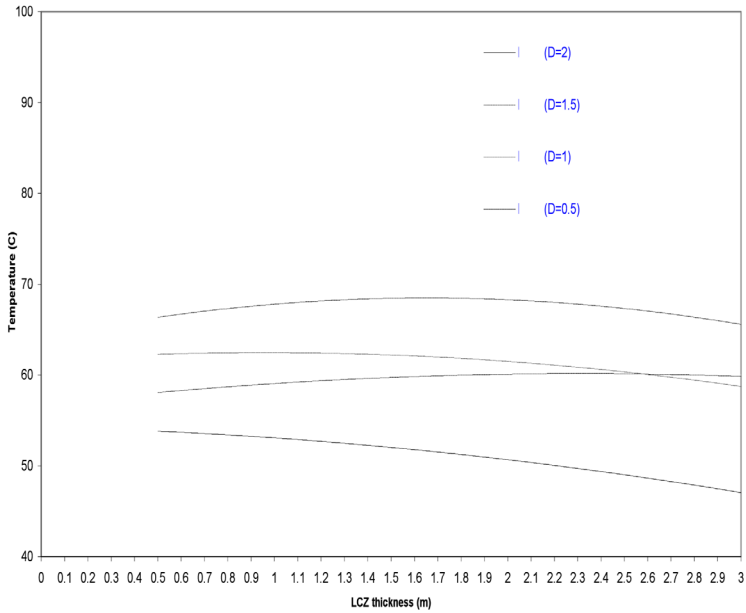

Figure 10. The energy still available in the loaded pond

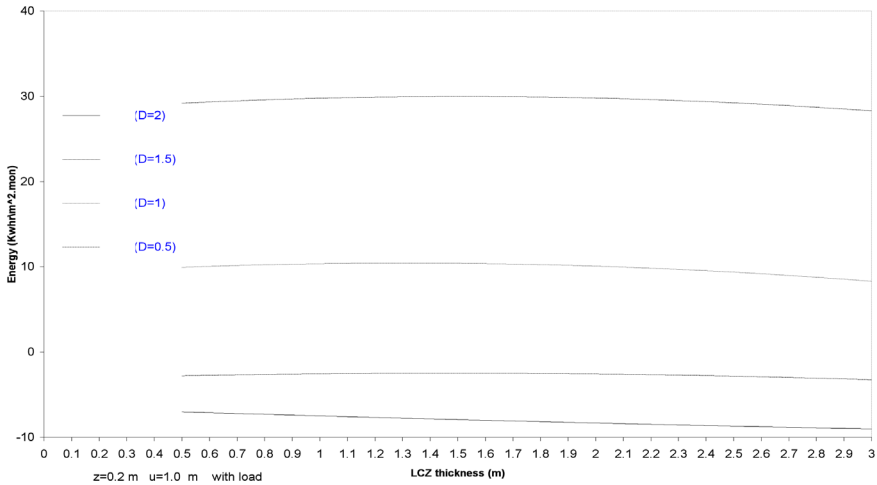

Figure 11. The average annual storage zone temperature vs. NCZ thickness for different applied load (Z1=0.2m, Ds=1.0m)

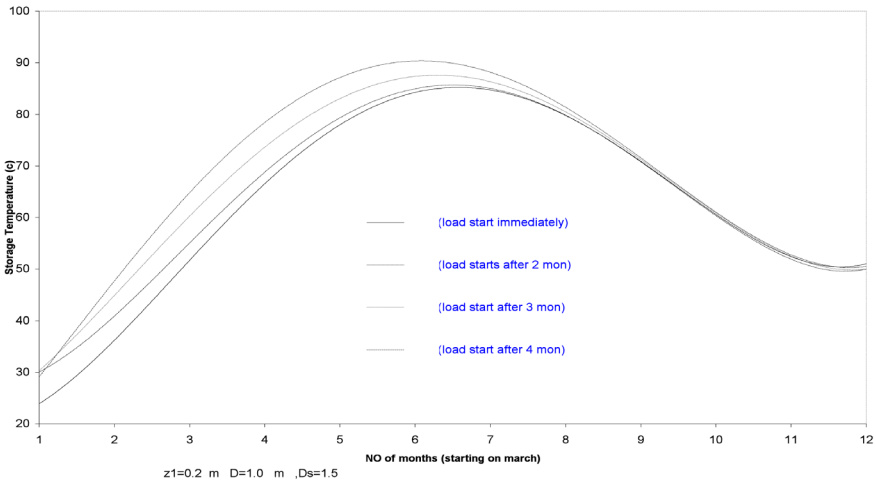

Figure 12. The effect of the load on the transient energy gain (Z1=0.2m, Ds=1.5m, D=1.0m)

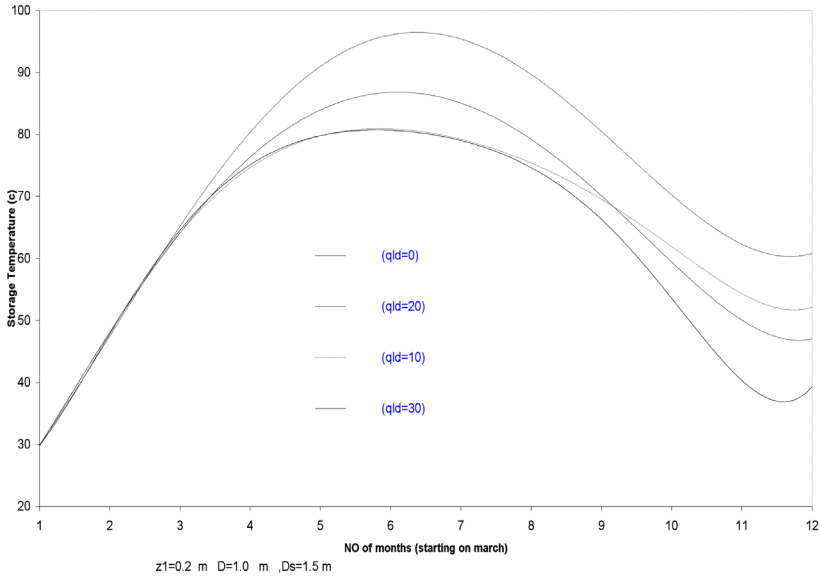

Figure 13. The effect of the load on the loosed energy from the LCZ (Z1=0.2m, Ds=1.5m, D=1.0m)

Figure 14. Dead Sea Solar Pond

CONCLUSIONS

The problem of the transient heat and mass transfer within a salt-gradient solar pond was investigated, with emphasis on the influence of the external factors on the stability characteristics. From the results obtained for a solar pond, the following conclusions were drawn:

- The solar radiation has an important effect on the internal temperature field and also on the pond stability characteristics.
- The critical zones appear to become more vulnerable to instabilities with the increase of time of operation.
- The solar heating effect and the heat losses from the free surface have an important influence on the pond stability characteristics in time.
- The lateral walls appear to be less susceptible to instabilities than the interior central areas of the pond.

References

[1] Abu-Hamatteh Z.S.H., Al-Jufout, Saleh2, Abbassi, B.3 and Besieso, M.S. "Biogas Energy: Unexplored Source of a Renewable Energy in Jordan" International Conference on Renewable Energies and Power Quality (ICREPQ'10) Granada (Spain), 23rd to 25th March, 2010.
[2] Tabor "Review Articles, Solar Ponds," *Solar Energy* 27, PP. 181-194 (1981).
[3] J. Hull, C. Neilsen and P. Golding, Salinity – Gradient Solar Pond, CRC, USA, 1989.
[4] Malek Kabariti, "Identification of National Energy Policies and Energy Access in Jordan," January 25, 2005, Energy Research Group
[5] S. Abughres, M. Mashena, and K. Agha, "Modeling the Performance of Solar Ponds," Center for Solar Energy Studies, Libya, 1989.
[6] Husain, M. "Computer simulation of salt gradient solar pond's thermal behaviour," *Renewable Energy*, 2003, Volume 28, Issue 5, Pages 769-802.
[7] Saleh, A. "Performance investigation of a salt gradient solar pond coupled with desalination facility near the Dead Sea," *Energy*, Volume 36, Issue 2, February 2011, Pages 922-931
[8] M.M. El-Refaee. "Numerical Simulation of the Performance of the Kuwait Experimental Salt-Gradient Solar Pond (KESGSP)," Energy Sources Part A Recovery Utilization and Environmental Effects, 1/1/1993
[9] Atkinson, J.F. "A wind-mixed layer model for solar ponds," *Solar Energy*, 1983, Volume 31, Issue 3, Pages 243-259
[10] R.S. Beniwal. "Thermal characteristics and performance of salt gradient solar ponds," *International Journal of Energy Research*, 07/1987
[11] Badran, A.A. "Numerical model for the behaviour of a salt-gradient solar-pond

Nomenclature

C Specific heat capacity of the brine	F Constant in equation
D Depth of the solar pond	hs Convective heat coefficient between the pond surface and the ambient air
d Thickness of the non-convecting zone (NCZ)=Z2-Z1	Hs Incident insulation at the pond surface
D' Declination of the sun	Hi A component of total radiation due to the transmitted radiation from the surface
Ds Thickness of the storage zone (LCZ) =Z3-Z2	HN Incident isolation reaching the storage zone
è Rate of evaporation of water at the pond surface	
K Thermal conductivity of the brine	Hr A component of total radiation due to the reflected radiation from the bottom
ks Coefficient of salt diffusivity	h(z) Pond transmition; fraction that is left at depth Z
kt Coefficient of thermal diffusivity	Hz Radiative energy reaching depth Z
n Refractive index	qz Heat conducted at
nd Number of day	depth Z
Br Prandtl number	S Salt concentration (salinity)
T Temperature	t Time
qe Heat transfer by evaporation at the pond surface	qc Convective heat transfer to the ambient air at the pond surface
Tsky Sky Temperature	Tamb Ambient temperature
Tgw Ground water temperature (sink temperature)	Tb Storage zone temperature
qld Heat extracted from the storage zone(load)	qr Infrared transfer to the ambient
Ulg Bottom loss conductors	U Total internal energy of the brine
V Air speed	Z Coordinate position (positive downward)
Z1 Thickness of UCZ	Z2 Depth of NCZ
α Bottom reflectivity	αc Thermal expansion coefficient
β Salt expansion coefficient	θr Refractive angle
β' Coefficient of transmission	θi Incident angle(solar zenith angle)
ε Water surface emissivity	δ Constant in equation
σ Stefan-Boltzman constant	ρ Density of the brine
τs The ratio of salt diffusivity to thermal diffusivity	υ Kinematics viscosity of the brine
φ Latitude angle (Inclination angle)	ω Hour angle
μ Extinction coefficient	
Subscript	
i denotes for position step	j denotes for time step

greenhouse-heating system," *Applied Energy*, 199709
[12] Haj Khalil, R.A. "Optimization of solar pond electrical power generation system," *Energy Conversion and Management*, Volume 38, Issue 8, May 1997, Pages 787-798
[13] Wang, Y.F. "A study on the transient behaviour of solar ponds," Energy, Volume 7, Issue 12, December 1982, Pages 1005-1017
[14] T. H. Kho. "DESIGN AND PERFORMANCE EVALUATION OF A SOLAR POND FOR INDUSTRIAL PROCESS HEATING," *International Journal of Sustainable Energy*, Volume 10, Issue 1 & 2 April 1991, pages 83 - 101
[15] http://matek.fazekas.hu/portal/tanitasianyagok/Kubatov_Antal/ErdMord/ErdMord.pdf
[16] Al-Jamal, K. "Effect of energy extraction on solar pond performance," *Energy Conversion and Management*, Volume 39, Issue 7, May 1998, Pages 559-566
[17] Angeli, C. "A one-dimensional numerical study of the salt diffusion in a salinity-gradient solar pond," *International Journal of Heat and Mass Transfer*, Volume 47, Issue 1, January 2004, Pages 1-10
[18] Wang, J. "Effect of water turbidity on thermal performance of a salt-gradient solar pond," *Solar Energy*, 199505
[19] Karakilcik, M. "Performance investigation of a solar pond," *Applied Thermal Engineering*, Volume 26, Issue 7, May 2006, Pages 727-735
[20] Al-Jamal, K. "Parametric study of a solar pond for Northern Jordan," *Energy*, Volume 21, Issue 10, October 1996, Pages 939-946,
[21] Kamal, W.A. "A parametric study of the small-scale solar pond (SSSP)," Energy Conversion and Management, 1986, Volume 26, Issues 3-4, Pages 337-345.
[22] Srinivasan, J. "The effect of bottom reflectivity on the performance of a solar pond," *Solar Energy*, 1987
[23] Mansour, R.B. "Numerical study of transient heat and mass transfer and stability in a salt-gradient solar pond," *International Journal of Thermal Sciences*, Volume 43, Issue 8, August 2004, Pages 779-790

ABOUT THE AUTHOR

Mohammed Al-Dabbas is a mechanical engineer with a master's degree in oil shale combustion and a PhD in mathematical modeling of oil shale combustion. Dr. Al-Dabbas worked for Jordan's Ministry of Energy from 1992 until December 2004 in the renewable energy department as head of the oil shale section. He is currently an Assistant Professor in the Mechanical Engineering Department of Mutah University, Karak, Jordan. His research interests involve solar energy, wind, geothermal energy, oil shale combustion and hydrogen.